New Mexico Geological Society

Downloaded from: https://nmgs.nmt.edu/publications/guidebooks/70

Geochemistry of Capulin-phase Flows in the Raton-Clayton Volcanic Field

Frank C. Ramos, Matthew J. Zimmerer, Kate E. Zeigler, Sidney Pinkerton, and Nick Butterfield

2019, pp. 139-149. https://doi.org/10.56577/FFC-70.139

in:

Geology of the Raton-Clayton Area, Ramos, Frank; Zimmerer, Matthew J.; Zeigler, Kate; Ulmer-Scholle, Dana, New Mexico Geological Society 70 th Annual Fall Field Conference Guidebook, 168 p. https://doi.org/10.56577/FFC-70

This is one of many related papers that were included in the 2019 NMGS Fall Field Conference Guidebook.

Annual NMGS Fall Field Conference Guidebooks

Every fall since 1950, the New Mexico Geological Society (NMGS) has held an annual Fall Field Conference that explores some region of New Mexico (or surrounding states). Always well attended, these conferences provide a guidebook to participants. Besides detailed road logs, the guidebooks contain many well written, edited, and peer-reviewed geoscience papers. These books have set the national standard for geologic guidebooks and are an essential geologic reference for anyone working in or around New Mexico.

Free Downloads

NMGS has decided to make peer-reviewed papers from our Fall Field Conference guidebooks available for free download. This is in keeping with our mission of promoting interest, research, and cooperation regarding geology in New Mexico. However, guidebook sales represent a significant proportion of our operating budget. Therefore, only *research papers* are available for download. *Road logs*, *mini-papers*, and other selected content are available only in print for recent guidebooks.

Copyright Information

Publications of the New Mexico Geological Society, printed and electronic, are protected by the copyright laws of the United States. No material from the NMGS website, or printed and electronic publications, may be reprinted or redistributed without NMGS permission. Contact us for permission to reprint portions of any of our publications.

One printed copy of any materials from the NMGS website or our print and electronic publications may be made for individual use without our permission. Teachers and students may make unlimited copies for educational use. Any other use of these materials requires explicit permission.

This page is intentionally left blank to maintain order of facing pages.

New Mexico Geological Society Guidebook, 70th Field Conference, Geology of the Raton-Clayton Area, 2019, p. 139-149.

GEOCHEMISTRY OF CAPULIN-PHASE FLOWS IN THE RATON-CLAYTON VOLCANIC FIELD

Frank C. Ramos[1], Matthew J. Zimmerer[2], Kate E. Zeigler[3], Sidney Pinkerton[1], and
Nick Butterfield[1]

[1]Department of Geological Sciences, New Mexico State University, Las Cruces, NM 88003; framos@nmsu.edu
[2]New Mexico Bureau of Geology and Mineral Resources, Socorro, NM 87801; matthew.zimmerer@nmt.edu
[3]Zeigler Geologic Consulting, LLC, Albuquerque, New Mexico; zeiglergeo@gmail.com

Abstract — Capulin-phase basalts, trachybasalts, and trachyandesites of the Raton Clayton volcanic field erupted in the Folsom area of northeastern New Mexico between 54 and 37 ka have a range of compositional and isotopic signatures. Basalts and trachyandesites from Capulin Volcano define a separate suite that are likely associated through crystal fractionation and assimilation processes. High-MgO basalt erupted at Baby Capulin is least differentiated and best represents the trace element and isotope character of mantle underlying this region of the Great Plains, which is different than basalts erupted in the Rio Grande rift. Additional younger ~37 ka basalts erupted from Twin Mountain and Purvine Hills share strikingly similar major, trace element and isotope characteristics that may originate from eruptions that tapped the same magma chamber at different times.

INTRODUCTION

The Raton-Clayton volcanic field, located on the Great Plains in northeastern New Mexico at the eastern extent of the Jimez lineament (Fig. 1), encompasses three phases of volcanism that occurred from ~9 Ma to ~37 ka (Baldwin and Muehlebeger, 1959; Muehlberger et al., 1967; Stormer, 1972a; Scott and Pillmore, 1993; Mathis, 1997; Zimmerer, *this volume*). The first phase occurred between 9.0-3.5 Ma (or 3.6 Ma, Sayre and Ort, 2011) and is referred to as the Raton Phase. The second phase occurred between 3.0 and 2.3 Ma and is referred to as the Clayton phase. The third and youngest phase occurred between 1.7 Ma and 37 ka and is referred to as the Capulin phase. Capulin-phase basalts are typically associated with intact, minimally-eroded cinder cones best represented by Capulin Volcano. Basalts of the Capulin phase are also distinguished by having plagioclase phenocrysts and commonly hosting quartz xenocrysts (Stormer, 1972b). Although additional Capulin-phase flows are present to the south (e.g., Horseshoe Crater and Malpie Mountain), this contribution focuses on Capulin-phase flows located near the town of Folsom, New Mexico. Capulin-phase volcanics in this area include basalts, trachybasalts, and basaltic trachyandesites erupted from Capulin Volcano, Baby Capulin, Twin Mountain, Purvine Hills, or present at Folsom Falls. Many of these basalts share similar major and trace element characteristics but two sets of flows are notably different. Lavas at Capulin Volcano fall into two groups composed of less-evolved basalts (i.e., $SiO_2<50\%$) and more-evolved basaltic trachyandesites ($SiO_2>53\%$). In addition, at least one flow erupted from Baby Capulin is relatively primitive (i.e., MgO>10.3%) in comparison to all other Capulin-phase basalts. Here, we describe the geochemical characteristics of Capulin-phase basalts and petrogenetic groups defined by major elements, trace elements, and isotope ratios. These basalts offer one of the few opportunities in which to evaluate deep-sourced volcanism resulting from mantle melting under the Great Plains province of the western US.

Background

The Raton-Clayton volcanic field is located in the Great Plains province of the western US at the eastern termination of the Jemez lineament (Magnani et al., 2005), a zone of lithospheric weakness and the likely suture zone of the Yavapai and Matzatzal Proterozoic accreted terrains (Fig. 1). The Jemez lineament is marked by a series of aligned volcanic fields that stretch from Springerville Arizona to the Raton-Clayton area in northeastern New Mexico. Unlike regions to the west, lithospheric thickness underlying the Great Plains is extensive with

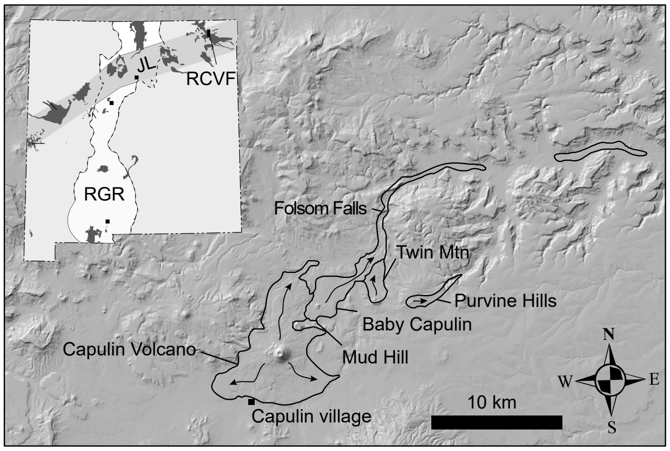

FIGURE 1. Location map showing Capulin-phase volcanic rocks of the Raton-Clayton volcanic field in northeastern New Mexico included in this study. Outline of flows from volcanic edifices are shown. The Folsom Falls sampling site and Mud Hill are also shown. Inset map shows Rio Grande rift (RGR), Jemez lineament (JL), and location of the Raton-Clayton volcanic field (RCVF).

crustal thickness exceeding 50 km (Wilson et al., 2005). Historically, the Raton-Clayton volcanic field has received little attention with most studies targeting age relationships with minimal associated petrologic understanding (e.g., Stormer, 1972a; Dungan et al., 1989). With recent $^{40}Ar/^{39}Ar$ dating (Table 1) using modern techniques and equipment (Zimmerer, *this volume*), Capulin-phase volcanic rocks are the target of renewed interest, as the Raton-Clayton volcanic field is the eastern-most site of Cenozoic volcanism in North America.

Unlike volcanic rocks generated during the Raton and Clayton phases of volcanism, many Capulin-phase basalts and trachyandesites host plagioclase crystals that confirm magmatic residence at crustal depths (<35 km; Ramos et al., 2005) where crustal assimilation was likely. Many of these plagioclase phenocrysts retain cloudy interiors (Stormer, 1972b), which are consistent with more complex petrogenetic histories. The additional common presence of quartz xenocrysts (Stormer, 1972b) is also consistent with this postulation. Capulin-phase volcanic rocks are both the youngest eruptions of the Raton-Clayton volcanic field and likely share similar petrogenetic histories, which may include crustal assimilation.

Recent dating using the $^{40}Ar/^{39}Ar$ technique determined the eruption ages of Capulin-phase volcanism in the Folsom area of northeastern New Mexico (Zimmerer, *this volume*). These new ages indicate that the oldest volcanism is represented by Capulin Volcano basalts, trachybasalts and trachyandesites at 54.2±1.8 ka. The next younger date originates from a flow from Baby Capulin sampled at Folsom Falls (Fig. 1) with a mean-weighted age 44.8±2.2 ka. The specific lava dated is thought to have high MgO (as compared to low-MgO lavas also emanating from Baby Capulin). Continued volcanism occurred at Twin Mountain and Purvine Hills with eruption ages of 36.7±2.3 ka and 36.6±6.0 ka, respectively. The ages of these flows overlap, indicating multiple flows were generated from at least two volcanic edifices at a similar or the same time.

Methods

Whole rocks of volcanic flows at Capulin Volcano, Baby Capulin, Twin Mountain, Purvine Hills, and Folsom Falls were collected in 2015 and 2016. Whole rocks were crushed using a jaw crusher and powdered using a shatterbox at New Mexico State University. Powders were then sent to the Peter Hooper GeoAnalytical Lab at Washington State University for analyses of major elements using X-ray fluorescence (XRF; Johnson et al., 1999) and trace elements using inductively coupled plasma mass spectrometry (ICP-MS; Jarvis, 1988).

Whole rock powders were also dissolved and analyzed for Sr, Nd, and Pb isotopes. Purification procedures followed those of Ramos (1992). Strontium isotopes were analyzed using seven Faraday collectors in multi-dynamic mode using a VG Sector thermal ionization mass spectrometer with Sr isotopes normalized to $^{86}Sr/^{88}Sr=0.1194$. Nd and Pb isotope were measured using seven collectors in static mode using a ThermoScientific Neptune multi-collector inductively coupled mass spectrometer with Nd isotopes normalized to $^{146}Nd/^{144}Nd=0.7219$ and Pb isotopes normalized to $^{203}Tl/^{205}Tl=0.41892$. All isotopes were measured at the Johnson Mass Spectrometry Laboratory at New Mexico State University.

Results

Capulin Volcano

The oldest (~54 ka) Capulin-phase volcanic rocks in the Folsom New Mexico area encompass compositions ranging from basalt to basaltic trachyandesite (Fig. 2; Table 2), where trachyandesites are present in the cone and basalts originate from flows emanating from the base of the cone. Whole rocks from Capulin Volcano define two distinct compositional groups that retain different major and trace element signatures (Figs. 2, 3, 4). Capulin Volcano basalts have lower SiO_2 and K_2O contents and lower incompatible trace elements characteristics than associated basaltic trachyandesites. Within the suite, K_2O increases ~30% (K_2O = ~1.4% to ~2.1%) with constant to decreasing Al_2O_3 contents (Fig. 3). In addition, MgO and Ni contents decrease (~7.4% to 5.6% and 123 to 87 ppm, respectively) in only a minor fashion. Ba concentrations also increase but Sr concentrations increase substantially less (Fig. 4).

Generally, Capulin Volcano basalts and basaltic trachyandesites have similar $^{87}Sr/^{86}Sr$ and $^{143}Nd/^{144}Nd$ isotope characteristics but different $^{206}Pb/^{204}Pb$ isotope characteristics (Fig. 5). $^{87}Sr/^{86}Sr$ ratios cluster at ~0.7041 and $^{143}Nd/^{144}Nd$ ratios are ~0.51267. The only significant deviation between basalts and trachyandesite whole rocks occurs in $^{206}Pb/^{204}Pb$ where ratios of basalts are ~17.56 and trachyandesites are more radiogenic (>17.59). Most other Pb isotope ratios are similar.

Baby Capulin

Similar to Capulin Volcano, basalts and basaltic trachyandesites erupted from Baby Capulin (44.8 ka) also define two compositional groups (Table 3). The first is highly magnesium (MgO>10%) with low SiO_2 contents. These basalts also have low K_2O and Al_2O_3 contents (Fig. 3). Incompatible element concentrations such as Ba and Sr are low and Ni and Cr contents are high, consistent with the primitive nature of this group (Fig. 4). Although three samples are presented, it is unclear if all three originate from a single eruption or multiple eruptions. The 44.8 ka Baby Capulin age (Table 1; Zimmerer, *this volume*) likely originates from a high-MgO Baby Capulin flow sampled at a different location (i.e., at Folsom Falls). High-MgO Baby Capulin basalts are dramatically different from all other basalts erupted in the Folsom area. They do however lie along trends in which other basalts are characterized by higher incompatible element concentrations and higher SiO_2 and Al_2O_3 contents (Figs. 3, 4).

In addition to primitive major and trace element compositions, high-MgO Baby Capulin basalts have both unradiogenic and radiogenic $^{87}Sr/^{86}Sr$ ratios that almost encompass the total range of ratios of Capulin-phase basalts (Fig. 5). In addition, $^{143}Nd/^{144}Nd$ ratios are similar and lower than more-evolved Baby Capulin basaltic trachyandesites. $^{206}Pb/^{204}Pb$ isotope ratios of these high MgO basalts also encompass most of the $^{206}Pb/^{204}Pb$ variation of Capulin-phase basalts but $^{207}Pb/^{204}Pb$ ratios are relatively constant.

TABLE 1. Table showing sample identifiers, vent sources, ages, compositions, and locations of Capulin-phase whole rocks.

Sample ID	Volcanic Center	Age (ka)*	Composition	Latitude	Longitude
SPC-11	Capulin	54.2±1.8	Basaltic Trachyand.	36.823	-103.939
SPC-12	Capulin	54.2±1.8	Basaltic Trachyand.	36.746	-103.962
SPC-18	Capulin	54.2±1.8	Basalt	36.786	-103.982
SPC-19	Capulin	54.2±1.8	Basalt	36.769	-103.999
SPC-20	Capulin	54.2±1.8	Basaltic Trachyand.	36.760	-103.992
NMRC-13	Capulin	54.2±1.8	Basalt	36.782	-103.970
NMRC-14	Capulin	54.2±1.8	Basalt	36.784	-103.990
NMRC-15	Capulin	54.2±1.8	Basalt	36.794	-103.966
NMRC-16	Capulin	54.2±1.8	Basalt	36.784	-103.979
SPC-1	Folsum Falls (BC or TW)	51.7±9.9	Basalt	36.906	-103.817
SPC-2	Folsum Falls (BC or TW)	51.7±9.9	Basalt	36.907	-103.830
SPC-3	Folsum Falls (BC or TW)	51.7±9.9	Basalt	36.901	-103.856
SPC-4	Folsum Falls (BC or TW)	51.7±9.9	Basalt	36.893	-103.866
SPC-5	Folsum Falls (BC or TW)	51.7±9.9	Basalt	36.881	-103.873
SPC-6	Folsum Falls (BC or TW)	51.7±9.9	Basalt	36.881	-103.871
SPC-8	Baby Capulin	44.8±2.2	Basalt	36.812	-103.937
SPC-9	Baby Capulin	44.8±2.2	Basaltic Trachyand.	36.814	-103.939
SPC-10	Baby Capulin	44.8±2.2	Basaltic Trachyand.	36.817	-103.933
SPC-34	Baby Capulin	44.8±2.2	Basalt	36.819	-103.925
SPC-35	Baby Capulin	44.8±2.2	Basalt	36.820	-103.921
SPC-13	Twin Mountain	36.7±2.3	Basaltic Trachyand.	36.820	-103.880
SPC-14	Twin Mountain	36.7±2.3	Basalt	36.810	-103.888
SPC-15	Twin Mountain	36.7±2.3	Basalt	36.819	-103.891
SPC-16	Twin Mountain	36.7±2.3	Basalt	36.826	-103.882
SPC-17	Twin Mountain	36.7±2.3	Basalt	36.834	-103.895
JS-95-48	Twin Mountain	36.7±2.3	Basalt	36.822	-103.888
SPC-26	Purvine Hills	36.6±6.0	Basalt	36.816	-103.859
SPC-27	Purvine Hills	36.6±6.0	Basalt	36.816	-103.858
SPC-28	Purvine Hills	36.6±6.0	Basalt	36.816	-103.855
SPC-29	Purvine Hills	36.6±6.0	Basalt	36.816	-103.851

*Ages from Zimmerer *this volume.*

In contrast to the high MgO group, a second group of basaltic trachyandesites is characterized by lower-MgO (MgO= ~6.6%) contents at Baby Capulin. These basalts have higher SiO_2 and Al_2O_3 contents and higher K_2O and incompatible trace element contents (Figs. 2, 3). This group is more evolved and retains similar compositions as basalts erupted at Twin Mountain, Purvine Hills, and those sampled at Folsom Falls.

The isotopic nature of this group of Baby Capulin basaltic trachyandesites is also different. $^{87}Sr/^{86}Sr$ ratios are more radiogenic than high-MgO Baby Capulin basalts and are similar to those of Twin Mountain basalts (Fig. 5). $^{143}Nd/^{144}Nd$ ratios are also more radiogenic than the high-MgO Baby Capulin basalts. In contrast, Pb isotope ratios are intermediate between high-MgO basalts but are still similar to Pb isotope ratios of basalts at Folsum Falls.

Twin Mountain, Folsom Falls, and Purvine Hills

Basalts from Twin Mountain (37 ka) and basalts sampled at Folsom Falls (i.e., erupted at other sites but sampled at the Folsom Falls site) have similar major and trace element compositions (Tables 4, 5). These basalts also share similar geochemical characteristics as more-evolved, low-MgO Baby Capulin basaltic trachyandesites. The major and trace element compositions of these basalts are also very similar to the major and trace element compositions of basalts erupted from Purvine Hills (36.6 ka; Table 6). As such, SiO_2 contents of these basalts range from 51-53% with Al_2O_3 and K_2O contents ranging from 16 to 17% and 1.0 to 1.5%, respectively (Fig. 3). Trace element compositions are also relatively uniform with Nb, Ba, and Sr ranging from 16 to 20 ppm, 450 to 650 ppm, and 550 to 650 ppm, respectively (Fig. 4).

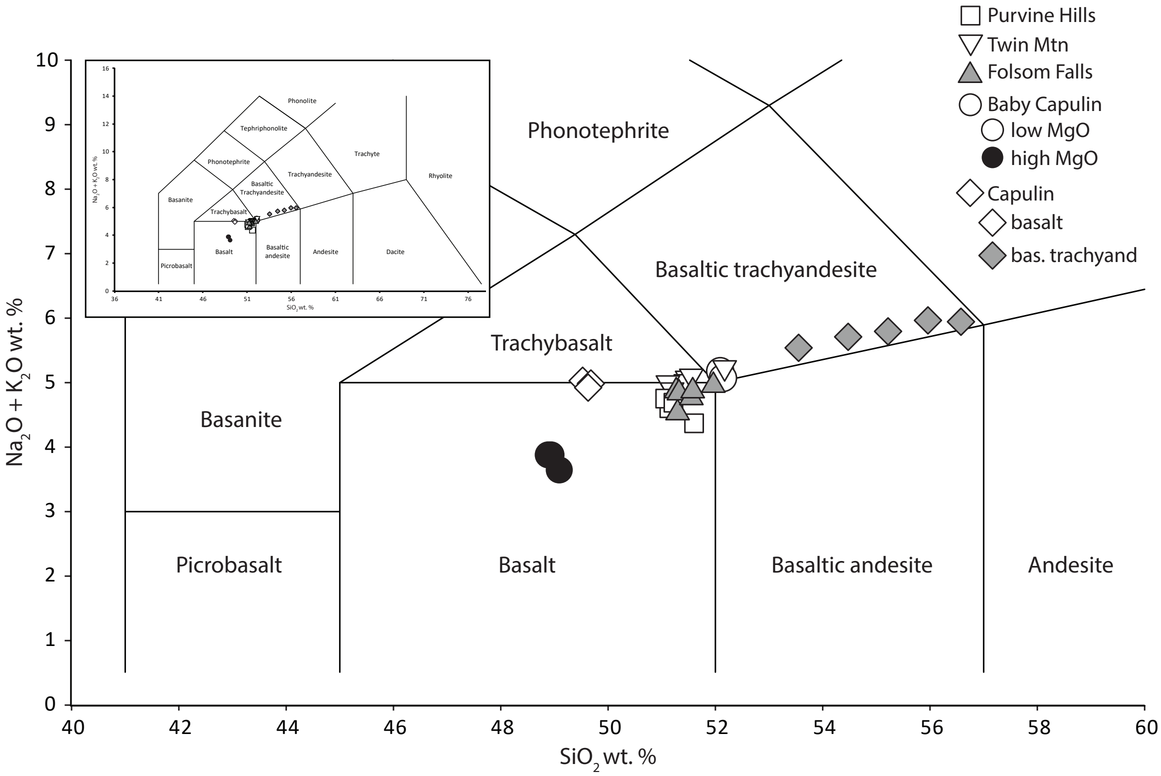

FIGURE 2. Total-alkali versus silica diagram showing Capulin-phase volcanic rocks from the Folsom New Mexico area. Note the range of compositions encompassed by 54-37 ka volcanic rocks in the region.

This same suite of basalts also shares similar isotopic characteristics although some outliers exist (Fig. 5). $^{87}Sr/^{86}Sr$ ratios range from ~0.7039 to 0.7041, while $^{143}Nd/^{144}Nd$ ratios are largely within analytical reproducibility at 0.51268 to 0.51272. Lead isotope ratios reflect greater variation with $^{206}Pb/^{204}Pb$ ranging from ~17.58 to 17.65 and $^{207}Pb/^{204}Pb$ ranging from ~15.45 to 15.49. Basalts from Purvine Hills are somewhat distinctive however in that they retain $^{143}Nd/^{144}Nd$ ratios lower than 0.51268 (Fig. 5).

DISCUSSION

Major element, trace element, and isotopic variations of Capulin-phase basalts and trachyandesites in the Folsom area are largely correlated with eruption age. Capulin-phase basalts also host plagioclase phenocrysts, which is consistent with magmatic staging at crustal depths during ascent (e.g., Ramos et al., 2005). The additional presence of cloudy plagioclase crystals and common occurrence of quartz xenocrysts (Stormer, 1972b) is consistent with magmatic interaction with silica-rich crustal lithologies prior to eruption. As such, the following discussion addresses magmatic evolution and characteristics in chronological order.

Early Capulin-phase eruptions at Capulin Volcano are distinctive and range from basaltic to trachyandesitic compositions. Compositions of early-erupted basalts in the region are relatively evolved (i.e., MgO = 7.1 to 7.4) with intermediate Al_2O_3 and K_2O contents (Fig. 3). These basalts have high $^{87}Sr/^{86}Sr$ ratios (>0.7041) compared to other basalts in the area. They also have intermediate $^{143}Nd/^{144}Nd$ ratios and the least radiogenic $^{206}Pb/^{204}Pb$ ratios of basalts erupted in the Folsom area. In contrast, more-evolved, Capulin Volcano trachyandesites have higher SiO_2, lower Al_2O_3, higher K_2O and higher incompatible element concentrations consistent with more extensive crystal fractionation (Figs. 3, 4). These characteristics are coupled with less radiogenic $^{87}Sr/^{86}Sr$, constant $^{143}Nd/^{144}Nd$, and more radiogenic $^{206}Pb/^{204}Pb$ ratios compared to Capulin Volcano basalts. Taken together, these geochemical and isotopic traits likely result from continued fractionation of olivine and plagioclase and, in part, accompanying assimilation. Thus, changing isotope ratios to less radiogenic $^{87}Sr/^{86}Sr$ and more radiogenic $^{206}Pb/^{204}Pb$ may reflect effects resulting from open-system behavior and the end-members involved. Variable trace element enrichments of highly incompatible elements such as Sr and Ba (Fig. 4) also likely result from crustal assimilation accompanying fractionation. The additional presence of plagioclase, including cloudy plagioclase crystals (Stormer, 1972b), suggests that Capulin Volcano basaltic and basaltic trachyandesitic magmas differentiated at crustal levels where assimilation likely occurred, which was also responsible for the additional presence of quartz xenocrysts.

In contrast to Capulin Volcano basalts, high-MgO basalts erupted at Baby Capulin reflect the most primitive Capulin-phase magmatic compositions erupted in the Folsom area. These high-MgO basalts are inconsistent with extensive differentiation or open-system modification and retain MgO contents >10%, high Ni contents, and low Al_2O_3 contents. Their minimally differentiated nature offers the best opportunity to constrain

TABLE 2. Major and trace elements of Capulin Volcano whole rocks.

Sample ID	CAP SPC11	CAP SPC12	CAP SPC18	CAP SPC19	CAP SPC20	NMRC-13	NMRC-14	NMRC-15	NMRC-16
XRF major element oxides normalized to 100%									
SiO^2	56.60	55.24	54.49	53.57	55.97	49.54	49.64	49.69	53.57
TiO^2	1.11	1.17	1.18	1.22	1.12	1.45	1.47	1.44	1.22
Al_2O_3	15.78	15.91	15.99	15.89	15.92	16.11	16.29	15.95	15.89
FeO*	7.48	8.00	8.34	8.67	7.75	10.27	10.42	10.33	8.67
MnO	0.13	0.13	0.14	0.15	0.13	0.17	0.17	0.17	0.15
MgO	5.55	6.10	5.76	6.37	5.61	7.3	7.07	7.38	6.37
CaO	7.09	7.25	7.90	8.10	7.13	9.60	9.49	9.50	8.10
Na_2O	3.8	3.8	3.81	3.71	3.85	3.65	3.57	3.63	3.71
K_2O	2.14	1.99	1.9	1.82	2.12	1.37	1.35	1.36	1.82
P_2O_5	0.42	0.41	0.49	0.51	0.42	0.55	0.52	0.56	0.51
Total	100	100	100	100	100	100	100	100	100
XRF trace elements (ppm)									
Ni	97	104	87	110	91	114	123	118	120
Ba	894	839	905	861	900	703	700	697	624
Rb	30.4	29.0	26.9	25.8	30.0	18.04	17.5	17.7	19.0
Sr	711	690	808	828	718	857	862	847	757
Zr	155	155	157	158	154	152	154	153	152
Y	19.2	19.8	21.5	22.5	19.5	24.38	23.1	23.3	22.7
Nb	27.7	26.9	27.6	26.6	28.0	?	24.67	25.6	26.7
La	37.0	35.6	42.1	42.2	37.5	38.4	36.6	39.68	34.8
Ce	65.7	64.2	76.3	77.1	66.6	71.5	65.6	72.1	57.81
Th	6.9	6.4	6.82	6.2	7.08	4.7	4.7	5.17	4.07
Nd	26.6	26.5	31.1	32.7	27.0	31.98	28.86	31.49	28.6
U	2.28	2.09	2.14	1.88	2.38	2.13	1.92	1.21	1.84
Pr	7.27	7.17	8.57	8.78	7.44	8.62	7.33	8.34	7.53
Sm	4.97	4.95	5.80	6.02	5.01	5.92	5.23	5.89	5.01
Eu	1.55	1.57	1.78	1.81	1.58	1.74	1.56	1.79	1.59
Gd	4.32	4.37	4.87	5.18	4.40	5.12	4.33	4.98	4.39
Tb	0.66	0.69	0.75	0.79	0.67	0.74	0.67	0.77	0.69
Dy	3.85	4.01	4.43	4.45	3.79	4.12	3.84	4.43	3.81
Ho	0.76	0.79	0.85	0.87	0.75	0.84	0.77	0.86	0.76
Er	1.99	2.07	2.21	2.28	2.00	2.2	2.05	2.27	2.08
Tm	0.28	0.29	0.31	0.33	0.29	0.3	0.28	0.32	0.29
Yb	1.73	1.74	1.89	1.94	1.7	1.93	1.75	1.91	1.72
Lu	0.26	0.27	0.28	0.30	0.28	0.28	0.27	0.29	0.28
Hf	3.68	3.69	3.72	3.77	3.68	3.7	3.68	3.74	3.68
Ta	1.88	1.83	1.79	1.70	1.89	1.76	1.87	1.78	1.84
Cs	0.58	0.54	0.54	0.46	0.57	0.54	0.56	0.48	0.57
Sc	18.2	19.5	20.3	20.9	18.4	20.8	18.7	19.8	18.8
$^{87}Sr/^{86}Sr$	0.70412	0.70411	0.70411	0.70412	0.70413	0.70415	0.70421	0.70413	0.70402
$^{143}Nd/^{144}Nd$	0.51268	0.51268	0.51267	0.51266	0.51267	0.51268	0.51269	0.51268	0.51271
$^{206}Pb/^{204}Pb$	17.618	17.620	17.596	17.624	17.605	17.574	17.559	17.563	17.723
$^{207}Pb/^{204}Pb$	15.468	15.464	15.471	15.495	15.464	15.470	15.459	15.466	15.485
$^{208}Pb/^{204}Pb$	37.345	37.339	37.336	37.390	37.327	37.303	37.270	37.284	37.437

Whole rocks were generated from hand-picked gravels. Isotope ratios are not age corrected. Iron was measured as total Fe (FeO*). Strontium isotopes were analyzed using TIMS and Nd and Pb were analyzed using MC-ICP-MS at NMSU. NBS987 Sr standard results were 0.710293 (n=37) with 0.000033 SD, JNdi-1 results were 0.512093 (n=44) with 0.000008 SD; and NBS981 results were $^{206}Pb/^{204}Pb$=16.929 (n=59) with a 0.003 SD, $^{207}Pb/^{204}Pb$=15.482 (n=59) with a 0.003 SD, $^{208}Pb/^{204}Pb$=36.668 (n=59) with a 0.010 SD for the six months surrounding the actual period of analyses. NBS987 analyzed with the samples was $^{87}Sr/^{86}Sr$= 0.710281, n=2. Similarly, JNdi-1 Nd standard was $^{143}Nd/^{144}Nd$: 0.512093, n=2 and $^{145}Nd/^{144}Nd$: 0.348406, n=2. NBS981 Pb standard ratios were $^{206}Pb/^{204}Pb$: 16.931, n=2; $^{207}Pb/^{204}Pb$: 15.485, n=2, and $^{208}Pb/^{204}Pb$: 36.677, n=2.

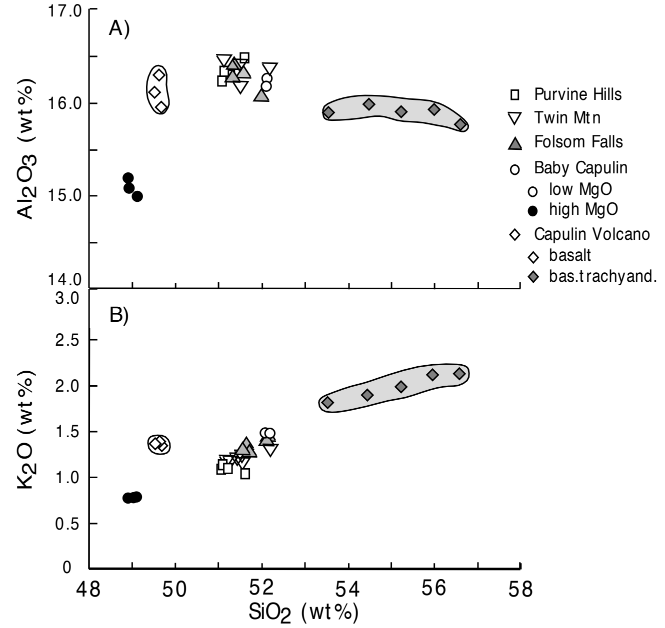

FIGURE 3. Harker diagrams showing **A**) SiO_2 and Al_2O_3 variations, and **B**) SiO_2 and K_2O variations of Capulin-phase volcanic rocks. Note differences in compositions of Capulin volcano basalts and trachyandesites compared to other Capulin-phase volcanic rocks.

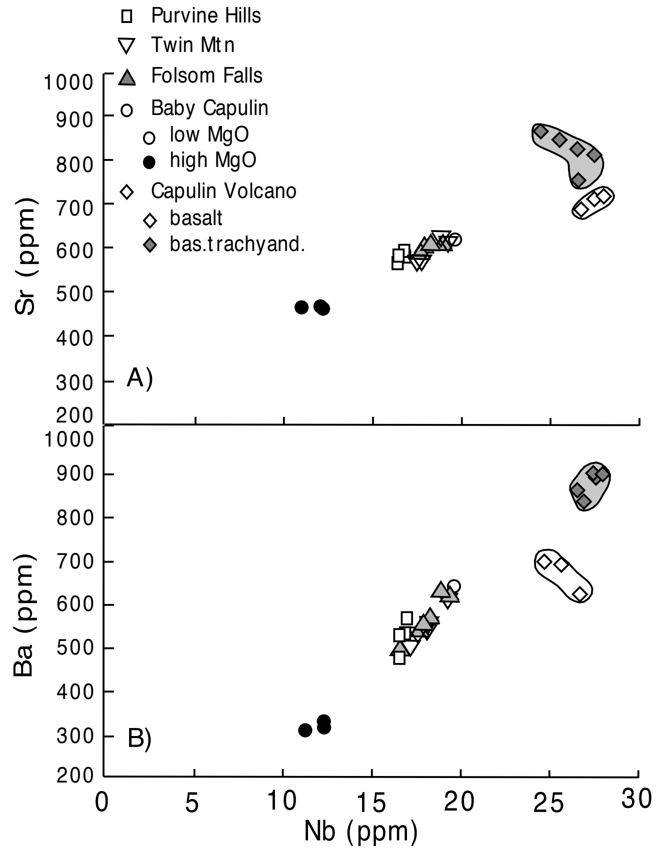

FIGURE 4. Trace element variation diagrams showing **A**) niobium and strontium variations, and **B**) niobium and barium variations of Capulin-phase Raton-Clayton basalts and trachyandesites. Capulin Volcano basalts and trachyandesite have the highest incompatible element concentrations, while high-MgO Baby Capulin basalts have the lowest incompatible element concentrations, and Twin Mountain and Purvine Hills basalts have intermediate concentrations.

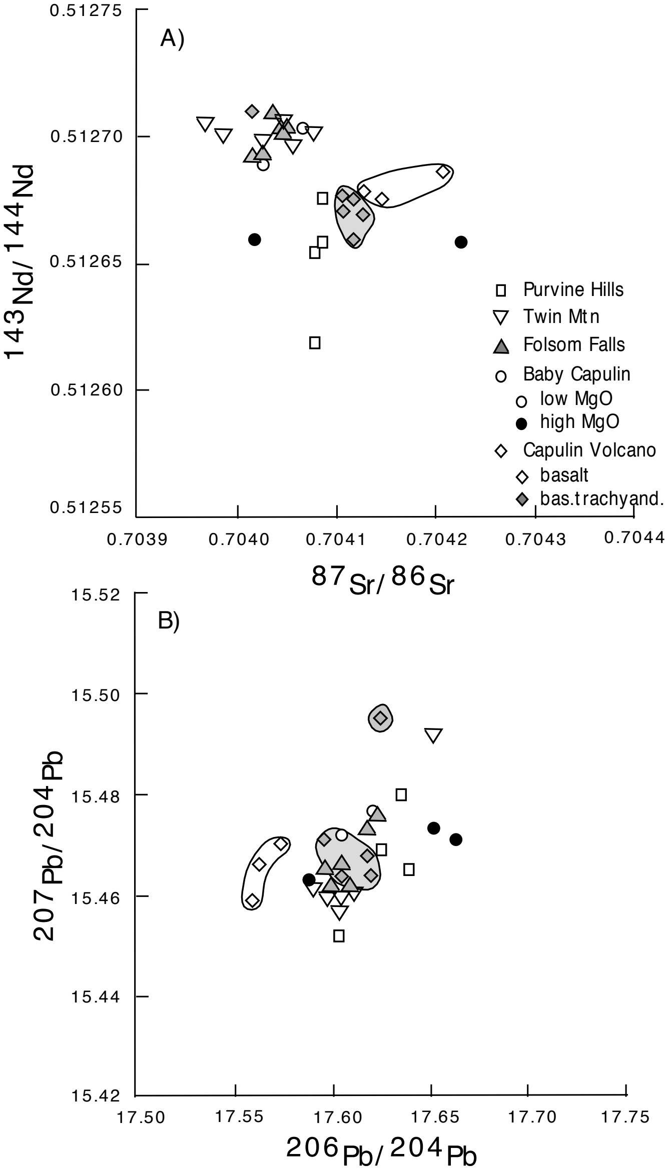

Figure 5. **A**) $^{87}Sr/^{86}Sr$-$^{143}Nd/^{144}Nd$ and **B**) $^{206}Pb/^{204}Pb$-$^{207}Pb/^{204}Pb$ isotope variation diagrams showing Capulin-phase volcanic rocks. Note variations between Capulin Volcano basalts and trachyandesites versus high-MgO content Baby Capulin basalts. Also shown are the similar compositions of Twin Mountain, Purvine Hills, and Folsom Falls basalts.

the geochemical and isotopic nature of mantle sources melted under this region of the Great Plains province. Besides having the highest MgO and lowest SiO_2 contents, high-MgO Baby Capulin basalts retain low incompatible element concentrations (e.g., Nb = 11-12 ppm; Sr = ~460 ppm), variable $^{87}Sr/^{86}Sr$ ratios, and variable $^{206}Pb/^{204}Pb$ ratios (Figs. 4, 5). They also retain less radiogenic $^{143}Nd/^{144}Nd$ ratios similar to selected basalts from Purvine Hills (Fig. 5). Despite their primitive nature, they still host olivine and plagioclase phenocrysts consistent with magmatic residence at crustal levels. As such, they could reflect a parental composition magma for all basalts erupted in the Folsom area or Raton-Clayton volcanic field more broadly.

Compared to high-MgO Baby Capulin basalts, low-MgO basaltic trachyandesites (~6.6 wt %) erupted from Baby Capu-

TABLE 3. Major and trace elements of Baby Capulin whole rocks.

Sample ID	BC SPC08	BC SPC09	BC SPC10	BC SPC34	BC SPC35
XRF major element oxides normalized to 100%					
SiO_2	49.12	52.12	52.15	48.91	48.96
TiO_2	1.31	1.39	1.39	1.34	1.36
Al_2O_3	15.00	16.17	16.26	15.19	15.08
FeO*	11.1	10.09	10.05	10.98	11.22
MnO	0.17	0.16	0.16	0.17	0.17
MgO	10.4	6.63	6.6	10.51	10.34
CaO	8.91	7.88	7.95	8.71	8.69
Na_2O	2.86	3.81	3.68	3.12	3.1
K_2O	0.77	1.37	1.38	0.76	0.77
P_2O_5	0.37	0.38	0.40	0.31	0.31
Total	100	100	100	100	100
XRF trace elements (ppm)					
Ni	274	113	112	272	258
Ba	311	618	643	319	334
Rb	8.63	18.5	17.0	8.4	8.6
Sr	466	603	619	469	464
Zr	108	145	146	116	118
Y	19.86	22.2	22.2	21.6	21.71
Nb	11.24	19.25	19.6	12.3	12.3
La	15.3	28.4	29.01	17.0	16.95
Ce	31.6	53.4	54.2	35.28	35.22
Th	1.4	4.0	4.1	1.54	1.57
Nd	16.49	23.95	24.07	18.3	18.1
U	0.42	1.24	1.29	0.45	0.48
Pr	4.0	6.24	6.36	4.43	4.39
Sm	3.87	4.9	5.00	4.22	4.25
Eu	1.39	1.6	1.63	1.47	1.45
Gd	4.07	4.67	4.7	4.39	4.36
Tb	0.67	0.76	0.76	0.72	0.73
Dy	4.01	4.55	4.5	4.33	4.44
Ho	0.8	0.89	0.87	0.85	0.88
Er	2.14	2.35	2.32	2.23	2.27
Tm	0.29	0.32	0.33	0.31	0.32
Yb	1.78	2.01	1.98	1.94	2.0
Lu	0.28	0.29	0.30	0.30	0.30
Hf	2.57	3.39	3.44	2.79	2.76
Ta	0.69	1.24	1.26	0.78	0.78
Cs	0.10	0.33	0.29	0.10	0.10
Sc	24.2	21.5	21.2	24.6	24.8
$^{87}Sr/^{86}Sr$	0.70423	0.70403	0.70407		0.70412
$^{143}Nd/^{144}Nd$	0.51266	0.51269	0.51270	0.51266	0.51266
$^{206}Pb/^{204}Pb$	17.588	17.621	17.605	17.652	17.663
$^{207}Pb/^{204}Pb$	15.463	15.476	15.472	15.473	15.471
$^{208}Pb/^{204}Pb$	37.317	37.339	37.321	37.270	37.278

Whole rocks were generated from hand-picked gravels. Isotope ratios are not age corrected. Iron was measured as total Fe (FeO*). Strontium isotopes were analyzed using TIMS and Nd and Pb were analyzed using MC-ICP-MS at NMSU. NBS987 Sr standard results were 0.710293 (n=37) with 0.000033 SD, JNdi-1 results were 0.512093 (n=44) with 0.000008 SD; and NBS981 results were 206Pb/204Pb=16.929 (n=59) with a 0.003 SD, 207Pb/204Pb=15.482 (n=59) with a 0.003 SD, 208Pb/204Pb=36.668 (n=59) with a 0.010 SD for the six months surrounding the actual period of analyses. NBS987 analyzed with the samples was 87Sr/86Sr= 0.710281, n=2. Similarly, JNdi-1 Nd standard was 143Nd/144Nd: 0.512093, n=2 and 145Nd/144Nd: 0.348406, n=2. NBS981 Pb standard ratios were 206Pb/204Pb: 16.931, n=2; 207Pb/204Pb: 15.485, n=2, and 208Pb/204Pb: 36.677, n=2.

lin are significantly more evolved. They have higher SiO_2, Al_2O_3, K_2O, and incompatible element concentrations (Figs. 3, 4). They also retain geochemical characteristics that are very similar to basalts erupted from Twin Mountain and Purvine Hills. Thus, their origins are addressed in relation to basalts from Twin Mountain and Purvine Hills.

Basalts erupted at Twin Mountain (37 ka), Purvine Hills (37 ka), and basalts sampled at Folsom Falls, which likely erupted from these sites or Baby Capulin, have intermediate SiO_2 compositions, higher Al_2O_3 contents, and intermediate K_2O contents (Figs. 2, 3). They also have intermediate trace element concentrations (Fig. 4). These basalts, and low-MgO Baby Capulin basaltic trachyandesites, have strikingly similar major and trace element compositions that may result from magmas tapped from the same chamber. They also uniformly have plagioclase phenocrysts that suggest magmatic staging at crustal levels (<35 km). Their youth suggests that they best represent the last stages of Capulin basaltic volcanism that resulted from more extensive differentiation from high-MgO, Baby Capulin basalts. Purvine Hills basalts retain somewhat different isotopic signatures compared to other Capulin-phase basalts. In their case, Purvine basalts have less radiogenic $^{143}Nd/^{144}Nd$ ratios and higher $^{206}Pb/^{204}Pb$ ratios (Fig. 5) that could result from melting subtly different mantle sources or assimilating different crustal materials.

Compared to young (<11 Ma) basalts erupted in the Rio Grande rift (McMillan et al., 2000), Capulin-phase basalts and basaltic andesites retain isotopic characteristics that are largely inherited from different mantle sources. In general, young Rio Grande rift basalts have radiogenic $^{143}Nd/^{144}Nd$ ratios and unradiogenic $^{87}Sr/^{86}Sr$ ratios while Capulin-phase basalts have unradiogenic $^{143}Nd/^{144}Nd$ ratios and moderately radiogenic $^{87}Sr/^{86}Sr$ (Fig. 6A). Capulin-phase basalts also have less radiogenic $^{206}Pb/^{204}Pb$ and $^{207}Pb/^{204}Pb$ ratios than young Rio Grande basalts (Fig. 6B), attesting to differences in the mantle generating basalts in this region of the Great Plains. Ultimately, Capulin-phase basalts likely originate from mantle that is different than that involved in magmagenesis in the Rio Grande rift.

CONCLUSIONS

Basalts of the Capulin-phase of the Raton-Clayton volcanic field erupted in the Folsom area of northeastern New Mexico reflect a range of mantle-derived compositions that staged at crustal levels prior to eruption. Early-erupted

TABLE 4. Major and trace elements of Twin Mountain whole rocks.

Sample ID	TM SPC13	TM SPC14	TM SPC15	TM SPC16	TM SPC17	TM JS 95-48
XRF major element oxides normalized to 100%						
SiO_2	52.19	51.47	51.2	51.49	51.14	51.56
TiO_2	1.43	1.40	1.49	1.46	1.43	1.49
Al_2O_3	16.38	16.19	16.35	16.41	16.47	16.34
FeO*	10.14	10.35	10.46	10.36	10.61	10.37
MnO	0.16	0.16	0.17	0.17	0.17	0.17
MgO	6.1	6.88	6.29	6.15	6.17	6.18
CaO	8.11	8.22	8.85	8.55	8.64	8.53
Na_2O	3.84	3.73	3.68	3.75	3.78	3.87
K_2O	1.34	1.23	1.15	1.26	1.15	1.17
P_2O_5	0.32	0.37	0.37	0.40	0.39	0.34
Total	100	100	100	100	100	100
XRF trace elements (ppm)						
Ni	81	122	77	72	76	68
Ba	615	548	511	559	546	538
Rb	17.99	16.3	14.4	15.3	12.2	14.8
Sr	612	582	576	601	606	587
Zr	147	140	141	144	146	139
Y	20.46	22.4	23.8	23.5	23.95	22.8
Nb	19.16	17.9	17.0	18.1	18.1	17.8
La	24.2	25.9	24.58	26.7	26.55	24.15
Ce	45.8	49.4	47.6	50.93	50.51	50.44
Th	3.7	3.4	2.86	3.28	3.18	2.81
Nd	20.94	22.5	22.76	23.7	23.9	21.3
U	1.14	1.05	0.89	0.97	0.91	1.75
Pr	5.4	5.87	5.78	6.08	6.05	5.84
Sm	4.46	4.87	4.95	5.04	5.12	4.97
Eu	1.58	1.6	1.68	1.7	1.73	1.67
Gd	4.27	4.64	4.95	4.93	4.97	4.93
Tb	0.68	0.75	0.8	0.81	0.8	0.79
Dy	4.23	4.48	4.79	4.8	4.86	4.76
Ho	0.82	0.89	0.96	0.93	0.96	0.91
Er	2.2	2.33	2.52	2.46	2.49	2.50
Tm	0.31	0.33	0.34	0.34	0.35	0.34
Yb	1.9	2.00	2.12	2.12	2.1	2.1
Lu	0.30	0.31	0.32	0.32	0.32	0.31
Hf	3.5	3.3	3.36	3.38	3.46	3.40
Ta	1.23	1.14	1.05	1.13	1.12	1.09
Cs	0.30	0.24	0.22	0.23	0.15	0.23
Sc	22.7	22.7	25.1	24.2	25.3	25.1
$^{87}\text{Sr}/^{86}\text{Sr}$	0.70406	0.70397	0.70404	0.70408	0.70403	0.70399
$^{143}\text{Nd}/^{144}\text{Nd}$	0.51270	0.51271	0.51271	0.51270	0.51270	0.51270
$^{206}\text{Pb}/^{204}\text{Pb}$	17.590	17.597	17.605	17.611	17.603	17.651
$^{207}\text{Pb}/^{204}\text{Pb}$	15.462	15.460	15.460	15.461	15.457	15.492
$^{208}\text{Pb}/^{204}\text{Pb}$	37.294	37.287	37.288	37.299	37.279	37.372

Whole rocks were generated from hand-picked gravels. Isotope ratios are not age corrected. Iron was measured as total Fe (FeO*). Strontium isotopes were analyzed using TIMS and Nd and Pb were analyzed using MC-ICP-MS at NMSU. NBS987 Sr standard results were 0.710293 (n=37) with 0.000033 SD, JNdi-1 results were 0.512093 (n=44) with 0.000008 SD; and NBS981 results were $^{206}\text{Pb}/^{204}\text{Pb}$=16.929 (n=59) with a 0.003 SD, $^{207}\text{Pb}/^{204}\text{Pb}$=15.482 (n=59) with a 0.003 SD, $^{208}\text{Pb}/^{204}\text{Pb}$=36.668 (n=59) with a 0.010 SD for the six months surrounding the actual period of analyses. NBS987 analyzed with the samples was $^{87}\text{Sr}/^{86}\text{Sr}$= 0.710281, n=2. Similarly, JNdi-1 Nd standard was $^{143}\text{Nd}/^{144}\text{Nd}$: 0.512093, n=2 and $^{145}\text{Nd}/^{144}\text{Nd}$: 0.348406, n=2. NBS981 Pb standard ratios were $^{206}\text{Pb}/^{204}\text{Pb}$: 16.931, n=2; $^{207}\text{Pb}/^{204}\text{Pb}$: 15.485, n=2, and $^{208}\text{Pb}/^{204}\text{Pb}$: 36.677, n=2.

basalts and basaltic trachyandesites (~54 ka) at Capulin Volcano have major and trace element compositions and isotopic characteristics that are different than other Capulin-phase basalts. These likely reflect the effects of crustal assimilation in addition to crystal fractionation. High-MgO basalts erupted from Baby Capulin at ~44 ka are primitive, reflect only minor amounts of fractionation, and best retain the geochemical characteristics of mantle underlying this region of the Great Plains. In contrast, basalts erupted from Twin Mountain and Purvine Hills at ~37 ka have similar signatures to basalts sampled at Folsom Falls and low MgO basalts erupted from Baby Capulin. These basalts also reflect greater amounts of fractionation and potential crustal assimilation and were likely generated from the same magma.

ACKNOWLEDGMENTS

This work was supported by a grant from the New Mexico Geological Society and by the Johnson Mass Spectrometry Laboratory at NMSU. Reviews by Gary Michelfelder and Sean Scott greatly improved the manuscript.

REFERENCES

Baldwin, B., and Muehlberger, W., 1959, Geologic studies of Union County, New Mexico: New Mexico Bureau of Mines and Mineral Resources Bulletin, v. 63, 171 p.

Dungan, M.A., Thompson, R. A., and Stormer, J.S., 1989, Rio Grande Rift volcanism: Northeastern Jemez zone, New Mexico: Field Excursions to volcanic terranes in the western United States, Vol 1: Southern Rocky Mountain Region: New Mexico Bureau of Mines and Mineral Resources Memoir 46, p. 474-475.

Jarvis, K. E., 1988, Inductively Coupled Plasma Mass-Spectrometry - a new technique for the rapid or ultra-trace level determination of the rare-earth elements in geological materials: Chemical Geology, v. 68, p. 31-39.

Johnson, D. M., Hooper P.R., and Conrey, R.M., 1999, XRF analysis of rocks and minerals for major and trace elements on a single low dilution Li-tetraborate fused bead: Advances in X-ray Analysis, v. 41, p. 843-867.

Magnani, M.B., Levander, A., Miller, K.C., Eshete, T., and Karlstrom, K.E., 2005, Seismic investigation of the Yavapai-Mazatzal transition zone and the Jemez Lineament in northeastern New Mexico: Geophysical Monograph Series, p. 227-238

Mathis, A., 1997, Geologist/Park Ranger at Capulin Volcano National Monument, personal communication and unpublished park interpretive materials.

TABLE 5. Major and trace elements of Folsom Falls whole rocks.

Sample ID	FF SPC01	FF SPC02	FF SPC03	FF SPC04	FF SPC05	FF SPC06
XRF major element oxides normalized to 100%						
SiO_2	51.32	51.59	51.99	51.28	51.56	51.35
TiO_2	1.481	1.451	1.385	1.473	1.458	1.469
Al_2O_3	16.25	16.46	16.06	16.32	16.31	16.38
FeO*	10.71	10.35	10.25	10.6	10.54	10.53
MnO	0.17	0.163	0.158	0.166	0.164	0.165
MgO	6.37	6.19	6.86	6.24	6.17	6.27
CaO	8.76	8.5	7.91	8.63	8.62	8.56
Na_2O	3.54	3.7	3.64	3.74	3.63	3.66
K_2O	1.04	1.22	1.36	1.17	1.19	1.24
P_2O_5	0.35	0.364	0.39	0.382	0.353	0.372
Total	100	100	100	100	100	100
XRF trace elements (ppm)						
Ni	77	78	125	78	75	75
Ba	503	571	628	540	562	562
Rb	10.4	13.99	17.77	13.73	14.52	15.09
Sr	565	609	604	595	609	603
Zr	138	144	144	142	143	144
Y	22.68	22.46	22.14	23.7	22.49	22.71
Nb	16.64	18.42	18.95	17.86	17.98	18.07
La	22.6	25.94	27.91	26.04	25.04	24.99
Ce	44.12	49.37	52.62	50.11	47.87	48.26
Th	2.69	3.4	3.82	3.11	3.15	3.17
Nd	21.11	22.75	23.7	23.39	22.35	22.35
U	0.83	1.02	1.2	0.92	1.06	0.97
Pr	5.31	5.89	6.16	6	5.74	5.78
Sm	4.68	4.84	4.85	4.99	4.77	4.72
Eu	1.62	1.67	1.63	1.73	1.65	1.6
Gd	4.64	4.68	4.59	4.92	4.75	4.73
Tb	0.76	0.76	0.76	0.81	0.77	0.77
Dy	4.62	4.52	4.44	4.85	4.62	4.57
Ho	0.93	0.89	0.89	0.95	0.89	0.92
Er	2.41	2.37	2.34	2.51	2.39	2.38
Tm	0.34	0.33	0.32	0.34	0.34	0.33
Yb	2.05	1.98	1.98	2.13	2	2.06
Lu	0.31	0.31	0.3	0.33	0.31	0.33
Hf	3.29	3.43	3.42	3.34	3.43	3.37
Ta	1.03	1.16	1.2	1.09	1.13	1.13
Cs	0.17	0.23	0.29	0.21	0.25	0.24
Sc	25.5	24.1	21.8	25.0	24.1	23.9
$^{87}Sr/^{86}Sr$	0.70405	0.70402	0.70405	0.70403	0.70404	0.70405
$^{143}Nd/^{144}Nd$	0.51270	0.51269	0.51270	0.51269	0.51271	0.51270
$^{206}Pb/^{204}Pb$	17.623	17.599	17.596	17.609	17.617	17.605
$^{207}Pb/^{204}Pb$	15.476	15.462	15.465	15.462	15.473	15.466
$^{208}Pb/^{204}Pb$	37.325	37.293	37.306	37.299	37.321	37.306

Whole rocks were generated from hand-picked gravels. Isotope ratios are not age corrected. Iron was measured as total Fe (FeO*). Strontium isotopes were analyzed using TIMS and Nd and Pb were analyzed using MC-ICP-MS at NMSU. NBS987 Sr standard results were 0.710293 (n=37) with 0.000033 SD, JNdi-1 results were 0.512093 (n=44) with 0.000008 SD; and NBS981 results were $^{206}Pb/^{204}Pb$=16.929 (n=59) with a 0.003 SD, $^{207}Pb/^{204}Pb$=15.482 (n=59) with a 0.003 SD, $^{208}Pb/^{204}Pb$=36.668 (n=59) with a 0.010 SD for the six months surrounding the actual period of analyses. NBS987 analyzed with the samples was $^{87}Sr/^{86}Sr$= 0.710281, n=2. Similarly, JNdi-1 Nd standard was $^{143}Nd/^{144}Nd$: 0.512093, n=2 and $^{145}Nd/^{144}Nd$: 0.348406, n=2. NBS981 Pb standard ratios were $^{206}Pb/^{204}Pb$: 16.931, n=2; $^{207}Pb/^{204}Pb$: 15.485, n=2, and $^{208}Pb/^{204}Pb$: 36.677, n=2.

Muehlberger, W.R., Baldwin, B., and Foster, R.W., 1967, High plains, northeastern New Mexico–Raton–Capulin Mountain–Clayton: New Mexico Bureau of Geology and Mineral Resources, Scenic Trips into the Geologic Past, 107 p.

McMillan, N.J., Dicken, A.P., and Hagg, D., 2000, Evolution of magma source regions in the Rio Grande rift, southern New Mexico: Geological Society of America Bulletin, v. 112, p. 1582-1593.

Ramos, F.C., 1992, Isotope geology of the Metamorphic Core of the Central Grouse Creek Mounrains, Box Elder County. Utah [MS thesis]: Los Angeles, University of California, 91 p.

Ramos, F.C., Wolff, J.A., and Tollstrup, D.L., 2005, Sr isotope disequilibrium in Columbia River flood basalts: Evidence for rapid shallow-level open-system processes: Geology, v. 33, p. 457-460.

Sayre, W.O., and Ort, M.H., 2011, A geologic study of the Capulin Volcano National Monument and surrounding areas, Union and Colfax Counties, New Mexico: New Mexico Bureau of Geology and Mineral Resources Open-file Report 541, 71 p.

Scott, G.R., and Pillmore, C.L., 1993, Geologic and structure-contour map of the Raton 30' x 60' Quadrangle, Colfax and Union counties, New Mexico, and Las Animas County, Colorado: U.S. Geological Survey Miscellaneous Investigations Series Map I-2266, scale 1:100,000.

Stormer, J.C., 1972a, Ages and nature of volcanic activity on the Southern High Plains, New Mexico and Colorado: Geological Society of America Bulletin, v. 83, p. 2443-2448.

Stormer, J.C., 1972b, Mineralogy and petrology of the Raton-Clayton Volcanic Field, Northeastern New Mexico: Geological Society of America Bulletin, v. 83, p. 3299-3322.

Wilson, D., Aster, R., Ni, J., Grand, S., West, W., Wei, G., Baldrige, W.S., and Smeken, S., 2005, Imaging the seismic structure of the crust and upper mantle beneath the Great Plains, Rio Grande Rift, and Colorado Plateau using receiver functions: Journal of Geophysical Research, v. 110, p. 1-14.

Zimmerer, M.J., 2019, $^{40}Ar/^{39}Ar$ geochronology, vent migration patterns, and hazard implications of the youngest eruptions in the Raton-Clayton volcanic field: New Mexico Geological Society, Guidebook 70, p. 151-160.

TABLE 6. Major and trace elements of Purvine Hills whole rocks.

Sample ID	PH SPC26	PH SPC27	PH SPC28	PH SPC29
XRF major element oxides normalized to 100%				
SiO_2	51.62	51.23	51.09	51.15
TiO_2	1.48	1.498	1.476	1.493
Al_2O_3	16.47	16.3	16.22	16.33
FeO*	10.56	10.65	10.55	10.65
MnO	0.168	0.169	0.169	0.17
MgO	6.29	6.39	6.51	6.47
CaO	8.66	8.75	8.89	8.83
Na_2O	3.34	3.6	3.62	3.5
K_2O	1.02	1.09	1.12	1.09
P_2O_5	0.392	0.309	0.343	0.322
Total	100	100	100	100
XRF trace elements (ppm)				
Ni	71	72	76	73
Ba	571	486	527	528
Rb	12.14	13.83	13.24	12.97
Sr	576	564	579	570
Zr	141	139	140	141
Y	23.99	21.97	22.5	22.5
Nb	16.94	16.62	16.85	16.64
La	25.07	21.06	22.32	21.72
Ce	48.04	41.33	43.83	42.8
Th	2.82	2.62	2.69	2.64
Nd	23.37	20.25	21.02	20.84
U	0.84	0.79	0.88	0.82
Pr	5.84	5.06	5.28	5.2
Sm	5.02	4.42	4.55	4.56
Eu	1.71	1.54	1.63	1.6
Gd	4.94	4.44	4.61	4.63
Tb	0.8	0.73	0.76	0.75
Dy	4.86	4.42	4.52	4.58
Ho	0.96	0.88	0.9	0.92
Er	2.53	2.37	2.39	2.4
Tm	0.36	0.33	0.33	0.34
Yb	2.18	1.99	2.04	2.06
Lu	0.34	0.31	0.31	0.32
Hf	3.27	3.37	3.26	3.35
Ta	1.07	1.06	1.05	1.07
Cs	0.19	0.21	0.19	0.21
Sc	25.2	25.3	25.2	25.7
$^{87}Sr/^{86}Sr$			0.70408	0.70409
$^{143}Nd/^{144}Nd$	0.51262	0.51266	0.51265	0.51268
$^{206}Pb/^{204}Pb$	17.625	17.635	17.603	17.639
$^{207}Pb/^{204}Pb$	15.469	15.480	15.452	15.465
$^{208}Pb/^{204}Pb$	37.307	37.332	37.263	37.307

Whole rocks were generated from hand-picked gravels. Isotope ratios are not age corrected. Iron was measured as total Fe (FeO*). Strontium isotopes were analyzed using TIMS and Nd and Pb were analyzed using MC-ICP-MS at NMSU. NBS987 Sr standard results were 0.710293 (n=37) with 0.000033 SD, JNdi-1 results were 0.512093 (n=44) with 0.000008 SD; and NBS981 results were $^{206}Pb/^{204}Pb$=16.929 (n=59) with a 0.003 SD, $^{207}Pb/^{204}Pb$=15.482 (n=59) with a 0.003 SD, $^{208}Pb/^{204}Pb$=36.668 (n=59) with a 0.010 SD for the six months surrounding the actual period of analyses. NBS987 analyzed with the samples was $^{87}Sr/^{86}Sr$= 0.710281, n=2. Similarly, JNdi-1 Nd standard was $^{143}Nd/^{144}Nd$: 0.512093, n=2 and $^{145}Nd/^{144}Nd$: 0.348406, n=2. NBS981 Pb standard ratios were $^{206}Pb/^{204}Pb$: 16.931, n=2; $^{207}Pb/^{204}Pb$: 15.485, n=2, and $^{208}Pb/^{204}Pb$: 36.677, n=2.

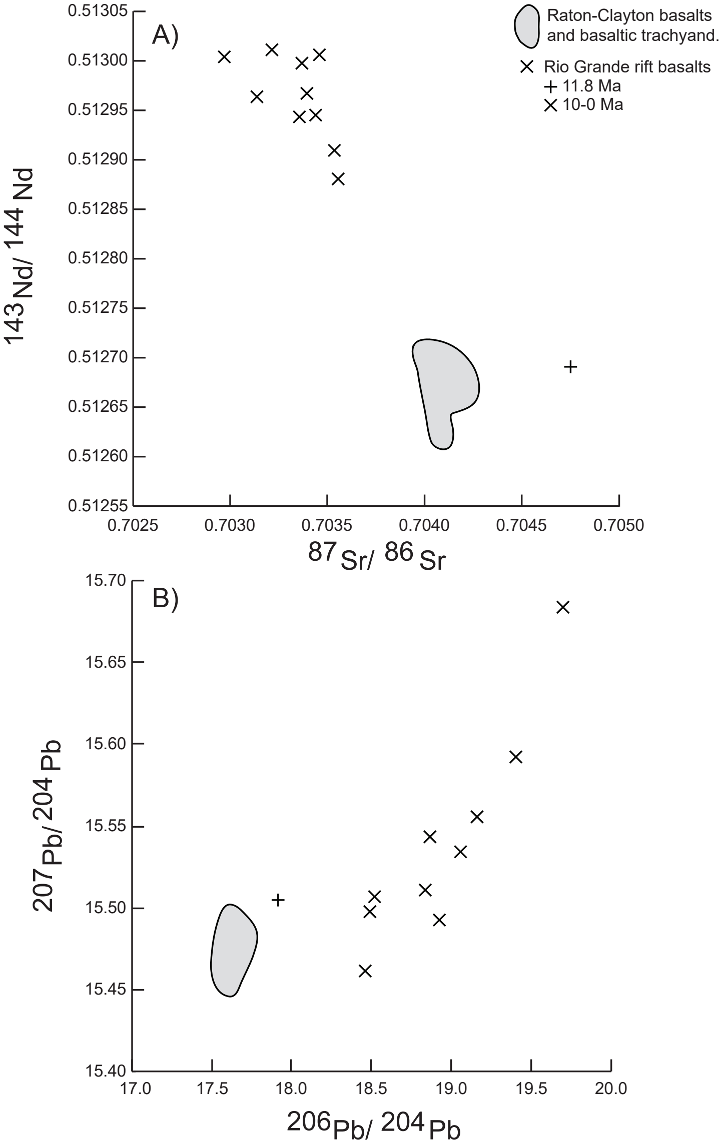

FIGURE 6. **A**) ^{87}Sr/^{86}Sr-^{143}Nd/^{144}Nd and **B**) ^{206}Pb/^{204}Pb-^{207}Pb/^{204}Pb isotope diagrams showing Raton-Clayton basalts and <11.8 Ma basalts from the Rio Grande rift. Note Raton-Clayton basalts have different isotope characteristics than most young basalts erupted in the Rio Grande rift (Rio Grande rift basalt isotope ratios from McMillan et al., 2000).